PHYSICAL REVIEW D **86,** 044027 (2012)

Black hole universe: Construction and analysis of initial data

Chul-Moon Yoo,[1,*] Hiroyuki Abe,[2,†] Yohsuke Takamori,[3,‡] and Ken-ichi Nakao[2,§]

[1]*Yukawa Institute for Theoretical Physics, Kyoto University, Kyoto 606-8502, Japan*

[2]*Department of Mathematics and Physics, Graduate School of Science, Osaka City University, 3-3-138 Sugimoto, Sumiyoshi, Osaka 558-8585, Japan*

[3]*Osaka City University Advanced Mathematical Institute, 3-3-138 Sugimoto, Sumiyoshi, Osaka 558-8585, Japan*

(Received 28 June 2012; published 15 August 2012)

We numerically construct an one-parameter family of initial data of an expanding inhomogeneous universe model which is composed of regularly aligned black holes with an identical mass. They are initial data for vacuum solutions of the Einstein equations. We call this universe model the ''black hole universe'' and analyze the structure of these initial data. We study the relation between the mean expansion rate of the 3-space, which corresponds to the Hubble parameter, and the mass density of black holes. The result implies that the same relation as that of the Einstein-de Sitter universe is realized in the limit of the large separation between neighboring black holes. The applicability of the cosmological Newtonian N-body simulation to the dark matter composed of black holes is also discussed. The deviation of the spatial metric of the cosmological Newtonian N-body system from that of the black hole universe is found to be smaller than about 1% in a region distant from the particles, if the separation length between neighboring particles is 20 times larger than their gravitational radius. By contrast, the deviation of the square of the Hubble parameter of the cosmological Newtonian N-body system from that of the black hole universe is about 20% for the same separation length.

DOI: 10.1103/PhysRevD.86.044027 PACS numbers: 98.80.Jk

I. INTRODUCTION

The homogeneous and isotropic universe model has enjoyed great success in explaining the observational data. By contrast, as anyone well knows, our universe is not exactly homogeneous and includes a lot of objects which serve as local nonlinear inhomogeneity. Usually, effects of local nonlinear structures on the global property of the universe are considered in an intuitive way or using some approximate methods. One of the effective ways to test the validity of our intuition or the approximation is to construct and study an exact or almost exact solution of the field equations, which may not be so realistic but should be able to fully describe nonlinear effects in an inhomogeneous universe model.

One example of exact inhomogeneous solutions is the so-called Swiss-cheese universe model [1,2]: the dust in an arbitrary number of nonoverlapping spherical regions is removed in a model of the homogeneous and isotropic universe filled with dust, and then each removed region is filled with a Schwarzschild black hole of the same mass as that of the removed dust. The remaining dust-filled region, which is corresponding to ''cheese,'' is playing the role of the glue to connect Schwarzschild patches. However, due to the existence of the cheese region, the Swiss-cheese model may be too special to see significant effects of local inhomogeneities on the global evolution of the universe. Hence, it is important to study a universe model in which black holes are uniformly distributed without the cheese region. We call such an inhomogeneous universe model the ''black hole universe'' in this paper.

About this issue, one innovative work was done by Lindquist and Wheeler in 1957 [3] and this work has been recently revisited in Refs. [4,5]. They divided a virtual 3-sphere into N cells ($N = 5$, 8, 16, 24, 120 and 600) and put a black hole portion of the Schwarzschild spacetime on a spherical region centered in each cell. Then they derived the equation of motion for this ''lattice universe'' from junction conditions between the Schwarzschild cell and the 3-sphere. It is demonstrated that the maximal radius of the lattice universe asymptotes to that of the corresponding homogeneous and isotropic closed universe filled with dust in the limit of the large number of black holes. Here we should note that the lattice universe is not an exact solution and there are gaps between each Schwarzschild black hole (see Fig. 3 in Ref. [3]).

Our purpose in this paper is to numerically construct initial data of the black hole universe. As a first step, we consider regularly aligned black holes with an identical mass. By its symmetry, no anisotropic relative velocities between neighboring black holes will appear, and this system is similar to a cold gas, i.e., dust. In order to obtain such initial data sets, we consider a black hole at the center of a cubic region and impose the periodic boundary conditions on its faces. A recipe for the initial data of the black hole universe and numerical procedure is given in Sec. II. The degree of inhomogeneity of the black hole universe is demonstrated in Sec. III A by calculating the traceless part

*yoo@yukawa.kyoto-u.ac.jp
†abe@sci.osaka-cu.ac.jp
‡takamori@sci.osaka-cu.ac.jp
§knakao@sci.osaka-cu.ac.jp

of the 3-dimensional Ricci curvature tensor of the initial hypersurface. The structure of the initial hypersurface is investigated in Sec. III B by searching for horizons.

One of the fascinating issues of inhomogeneous universe models is the so-called averaging problem. Naively, we expect that a universe model with local inhomogeneities, such as the black hole universe, can be globally described by a homogeneous universe model on average. However, the effect of local inhomogeneities on the global expansion definitely exists and the expansion history may be different from that of the homogeneous and isotropic universe [6–9]. This issue has been discussed a lot in past years (see reviews [10–12] and references therein), however there are few analyses which are applicable to inhomogeneous models with highly nonlinear metric inhomogeneity.[1] To solve this issue, we need to rely on numerical relativity. Our work may be the first step for the concrete analysis of the effects of nonlinear inhomogeneities in expanding universes. Although we cannot address the real time evolution of the black hole universe yet, the one-parameter family of initial data sets can be regarded as a fictitious time evolution of the black hole universe. Using the initial data sets, we study the cosmic volume expansion rate of the black hole universe model in Sec. III C.

The cosmological N-body simulation is a powerful tool for studying the structure formation in the universe by dealing with the motion of point particles, based on the cosmological Newtonian approximation. Since the interaction between these particles is the only gravity, the cosmological N-body simulation follows the time evolution of the dark matter in the cosmological context. The black hole is a candidate of the ingredient for the dark matter, and it is believed that the cosmological N-body simulation is applicable also to the black-hole dark matter. But it is a quite nontrivial issue whether the point particles in the cosmological N-body simulation can be simply identified with black holes. Hence, it is important to see in what situation the cosmological Newtonian N-body simulation is valid for the black hole universe. This issue is discussed in Sec. III D. Section IV is devoted to a summary.

In this paper, we use the geometrized units in which the speed of light and Newton's gravitational constant are one, respectively.

II. CONSTRUCTION OF INITIAL DATA FOR THE BLACK HOLE UNIVERSE

A. Constraint equations

In this paper, we are interested in the initial data of the vacuum Einstein equations. The initial data of the Einstein equations is equivalent to intrinsic and extrinsic geometries of a spacelike hypersurface, i.e., the intrinsic metric γ_{ij} and the extrinsic curvature K_{ij}, which represents how the spacelike hypersurface is embedded into the 4-dimensional spacetime. These are partially determined by the following four components of the Einstein equations:

$$\mathcal{R} + K^2 - K_{ij}K^{ij} = 0, \tag{1}$$

$$D_j K^j_i - D_i K = 0, \tag{2}$$

where $\mathcal{R}$ and D_i are Ricci curvature scalar and the covariant derivative with respect to the intrinsic metric γ_{ij}, respectively, and $K = \gamma^{ij}K_{ij}$. Equation (1) is called the Hamiltonian constraint, whereas Eq. (2) is called the momentum constraint.

Following an established procedure (see, e.g., Ref. [15]), we adopt the Cartesian spatial coordinate system and rewrite γ_{ij} and K_{ij} as

$$\gamma_{ij} = \Psi^4 \tilde{\gamma}_{ij}, \tag{3}$$

$$K^{ij} = \Psi^{-10}\left[\tilde{D}^i X^j + \tilde{D}^j X^i - \frac{2}{3}\tilde{\gamma}^{ij}\tilde{D}_k X^k + \hat{A}^{ij}_{\mathrm{TT}}\right] + \frac{1}{3}\Psi^{-4}\tilde{\gamma}^{ij}K, \tag{4}$$

where $\Psi := (\det\gamma_{ij})^{(1/12)}$, $\tilde{D}_i$ is covariant derivative with respect to the conformal metric $\tilde{\gamma}_{ij}$, and $\hat{A}^{ij}_{\mathrm{TT}}$ satisfies the transverse and traceless conditions,

$$\tilde{D}_j \hat{A}^{ij}_{\mathrm{TT}} = 0, \qquad \tilde{\gamma}_{ij}\hat{A}^{ij}_{\mathrm{TT}} = 0. \tag{5}$$

The conformal factor Ψ is determined so that the constraint equations are satisfied. The conformal metric $\tilde{\gamma}_{ij}$ has not six but five independent components due to the constraint $\det\tilde{\gamma}_{ij} = 1$. The three of the five components of $\tilde{\gamma}_{ij}$ can be always eliminated by the spatial coordinate transformation, and hence there are two physically meaningful components which can be freely chosen.

In the decomposition (4), mutually independent six components of K_{ij} are expressed by X^i, $\hat{A}^{ij}_{\mathrm{TT}}$ and K. The longitudinal traceless part composed of X^i is determined so that the constraint equations are satisfied, whereas the trace

[1] One of few exceptional examples was given in Ref. [13]. They studied the volume expansion rate of a kind of the Swiss-cheese model and showed that the cosmic volume expansion can be accelerated by nonlinear inhomogeneities. While we were writing this paper, Ref. [14] appeared. In Ref. [14], the authors analytically constructed N-body solutions of Einstein's constraint equations by considering regularly arranged distributions of discrete masses in topological 3-spheres. Significant differences between our present work and Ref. [14] are the spatial topology and the existence of the cosmic volume expansion. In our present case, the spatial topology is $\mathbf{T}^3$ with one point removed, and the expansion rate is finite while the initial data sets considered in Ref. [14] have a topology of $\mathbf{S}^3$ with N points removed, and their expansion rates vanish, i.e., time symmetric. One of the remarkable advantages of our work over Ref. [14] is that a dynamical simulation of an expanding universe is possible starting from our initial data, while only a contracting universe is possible with the initial data given in Ref. [14].

part K is related to the degree of freedom to choose the foliation of the spacetime by the family of spacelike hypersurfaces, or in other words, time slicing. By contrast, the transverse and traceless part $\hat{A}^{ij}_{\rm TT}$ has two independent components which can be freely chosen. These two components of $\hat{A}^{ij}_{\rm TT}$ and the physically meaningful two components of $\tilde{\gamma}_{ij}$ are usually regarded as physical degrees of freedom to set initial data for gravitational waves.

In order to avoid the cosmic volume expansion caused by artificial gravitational radiation, we assume trivial form of the conformal metric and no transverse and traceless part of the extrinsic curvature

$$\tilde{\gamma}_{ij} = \delta_{ij}, \tag{6}$$

$$\hat{A}^{ij}_{\rm TT} = 0, \tag{7}$$

where δ_{ij} is Kronecker's delta. As usual, we denote the inverse of $\tilde{\gamma}_{ij}$ by $\tilde{\gamma}^{ij}$ which is also equal to Kronecker's delta δ^{ij}. Then, Eqs. (1) and (2) are written as

$$\triangle \Psi + \frac{1}{8}(\tilde{L}X)_{ij}(\tilde{L}X)^{ij}\Psi^{-7} - \frac{1}{12}K^2\Psi^5 = 0, \tag{8}$$

$$\triangle X^i + \frac{1}{3}\partial^i\partial_j X^j - \frac{2}{3}\Psi^6\partial^i K = 0, \tag{9}$$

where $\triangle$ is the flat Laplacian, ∂_i is the ordinary derivative, and

$$(\tilde{L}X)^{ij} := \partial^i X^j + \partial^j X^i - \frac{2}{3}\delta^{ij}\partial_k X^k. \tag{10}$$

Here, note that $X_i := \tilde{\gamma}_{ij}X^j = X^i$ and $\partial^i := \tilde{\gamma}^{ij}\partial_j = \partial_i$, $(\tilde{L}X)_{ij} = \tilde{\gamma}_{ik}\tilde{\gamma}_{jl}(\tilde{L}X)^{kl} = (\tilde{L}X)^{ij}$, etc. We solve these equations by assuming an appropriate functional form of K as shown below.

B. Boundary condition and the trace of the extrinsic curvature

As mentioned above, we adopt the Cartesian coordinate system $\boldsymbol{x} = (x, y, z)$ and put a nonrotating black hole at the origin $\boldsymbol{x} = 0$ denoted hereafter by O. The black hole is represented by a structure like the Einstein-Rosen bridge in our initial hypersurface. Thus the origin O corresponds to the asymptotically flat spatial infinity and is often called the puncture. We focus on a cubic region $-L \le x \le +L$, $-L \le y \le +L$ and $-L \le z \le +L$ and call this region the domain $\mathcal{D}$. Since our aim is to construct the initial data of an expanding universe model with periodically aligned black holes, we impose the periodic boundary conditions; a point $\boldsymbol{x} = (-L, y, z)$ is identified with a point $\boldsymbol{x} = (+L, y, z)$, etc. Because of this boundary condition, the domain $\mathcal{D}$ is homeomorphic to the 3-torus $\mathbf{T}^3$. Since infinity is not included in the spacetime manifold, the initial hypersurface is $\mathcal{D}$ with O removed, which is denoted by $\mathcal{D}$-$\{O\}$, and thus it is homeomorphic to $\mathbf{T}^3$ with one point removed.[2] The covering space of $\mathcal{D}$-$\{O\}$ represents a cosmological model with regularly aligned black holes as shown in Fig. 1. Hereafter, we regard $\mathcal{D}$ as a cubic domain with boundary $\partial\mathcal{D}$ in the covering space.

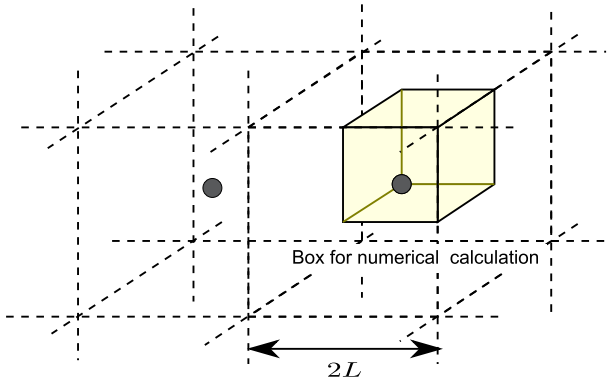

FIG. 1 (color online). The cubic region of our coordinates.

Here, we again note that the trace part of the extrinsic curvature K corresponds to the degree of freedom to choose the time slicing. In order to find the appropriate time slicing condition, first of all, we see the homogeneous and isotropic universe model. In this case, the expansion rate H which is called the Hubble parameter is related to the extrinsic curvature by

$$H = -\frac{1}{3}K. \tag{11}$$

The above relation implies that K of the expanding black hole universe model must be negative at least around the boundary of the cubic domain $\mathcal{D}$. By contrast, the maximal slicing condition $K = 0$ is appropriate for the foliation of the domain in the neighborhood of the asymptotically flat spatial infinity, and hence K should vanish in the vicinity of O (see Appendix).

Taking the above discussions into account, we assume

$$K(\boldsymbol{x}) = -3H_{\rm eff}W(R), \tag{12}$$

where $H_{\rm eff}$ is a positive constant which corresponds to the effective Hubble parameter, $R := |\boldsymbol{x}|$, and

$$W(R) = \begin{cases} 0 & \text{for } r\,0 \le R \le \ell \\ \sigma^{-36}[(R-\sigma-\ell)^6 - \sigma^6]^6 & \text{for } \ell \le R \le \ell + \sigma, \\ 1 & \text{for } \ell + \sigma \le R \end{cases} \tag{13}$$

ℓ and σ being constants which satisfy $\ell < \sigma < L$ (see Fig. 2).

[2]A similar configuration to our case was considered within the Lemaître-Tolman family of exact models in Refs. [16,17].

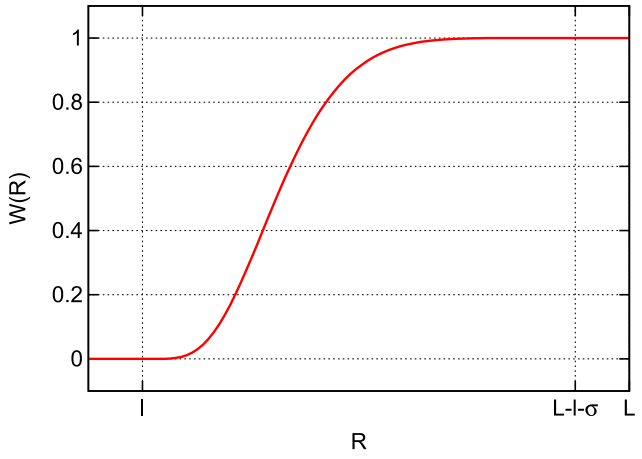

FIG. 2 (color online). The functional form of $W(R)$.

C. Extraction of the singularity at the center

Since K vanishes in the vicinity of the origin O, X^i and Ψ should behave as those of the Schwarzschild spacetime with the static isotropic coordinate system,

$$X^i \simeq 0, \tag{14}$$

$$\Psi \simeq \Psi_c + \frac{M}{2R}, \tag{15}$$

where Ψ_c and M are positive constants. Since Ψ itself is singular at O, we cannot handle Ψ numerically. Thus, instead of Ψ, we solve the constraint equations for the following new variable ψ:

$$\psi(\boldsymbol{x}) := \Psi(\boldsymbol{x}) - \frac{M}{2R}[1 - W(R)]. \tag{16}$$

Thanks to the second term proportional to $[1 - W(R)]$ in the right-hand side of the above equation, ψ is regular at O and satisfies the periodic boundary conditions.

The mass of a black hole is given by the Arnowitt-Deser-Misner (ADM) mass which is defined by the surface integral over the spacelike infinity at O. To see the ADM mass explicitly, we introduce a new radial coordinate

$$\tilde{R} = \frac{M^2}{4R}. \tag{17}$$

Then, by using a spherical polar coordinate system, the asymptotic form of the infinitesimal line element for $R \to 0$, or equivalently, $\tilde{R} \to \infty$, becomes

$$\mathrm{d}l^2 \simeq \left(\Psi_c + \frac{M}{2R}\right)^4 [\mathrm{d}R^2 + R^2(\mathrm{d}\theta^2 + \sin^2\theta \mathrm{d}\phi^2)] \tag{18}$$

$$= \left(1 + \frac{\Psi_c M}{2\tilde{R}}\right)^4 [\mathrm{d}\tilde{R}^2 + \tilde{R}^2(\mathrm{d}\theta^2 + \sin^2\theta \mathrm{d}\phi^2)]. \tag{19}$$

It is seen from the last equality of Eq. (19) that the mass of a black hole is given by $\Psi_c M$. Here note that there is a freedom of constant scaling of coordinates $\boldsymbol{x} \to C\boldsymbol{x}$. Using this freedom, we impose $\Psi_c = 1$, and thus the mass of a black hole is equal to M.

D. Hubble equation as an integrability condition

Integrating Eq. (8) over the physical domain $\mathcal{D}$-$\{O\}$, we obtain the following equation:

$$2\pi M + \frac{1}{8}\int_{\mathcal{D}\text{-}\{O\}} (\tilde{L}X)_{ij}(\tilde{L}X)^{ij}\Psi^{-7}\mathrm{d}x^3 - \frac{3}{4}H_{\mathrm{eff}}^2 V = 0, \tag{20}$$

where, by noting that the origin O can be regarded as the only boundary of $\mathcal{D}$-$\{O\}$ with the periodic boundary condition, the integral of $\Delta\Psi$ is rewritten as

$$\int_{\mathcal{D}\text{-}\{O\}} \Delta\Psi \mathrm{d}^3x = -\lim_{R\to 0}\int_0^{2\pi}\int_0^{\pi} \frac{\partial\Psi}{\partial R} R^2 \sin\theta \mathrm{d}\theta \mathrm{d}\phi = 2\pi M, \tag{21}$$

and we have defined V by

$$V := \int_{\mathcal{D}\text{-}\{O\}} W^2\Psi^5 \mathrm{d}^3x. \tag{22}$$

By rewriting Eq. (20), we have the effective Hubble equation as

$$H_{\mathrm{eff}}^2 = \frac{8\pi}{3}(\rho_{\mathrm{BH}} + \rho_{\mathrm{K}}), \tag{23}$$

where ρ_{BH} and ρ_{K} are defined by

$$\rho_{\mathrm{BH}} := \frac{M}{V}, \tag{24}$$

$$\rho_{\mathrm{K}} := \frac{1}{16\pi V}\int_{\mathcal{D}\text{-}\{O\}} (\tilde{L}X)_{ij}(\tilde{L}X)^{ij}\Psi^{-7}\mathrm{d}^3x. \tag{25}$$

Since V may be regarded as the effective volume of the expanding region, ρ_{BH} and ρ_{K} may be regarded as the mass density of black holes and the kinetic energy density of the spacetime, respectively. The effective Hubble equation gives a relation between two constants, the mass of the black hole M and the effective Hubble parameter H_{eff}, and, at the same time, it is an integrability condition of the constraint equations. How to guarantee this relation will be described in Sec. II F.

E. Momentum constraints

In this subsection, we rewrite the momentum constraints (9) into the numerically solvable forms. First, we define Z by

$$Z := \partial_i X^i. \tag{26}$$

Then, by taking the divergence of Eq. (9), we obtain

$$\triangle Z = \frac{1}{2}\partial_i(\Psi^6 \partial^i K). \tag{27}$$

Equation (9) is rewritten as

$$\triangle X^i = \frac{1}{3}\partial^i Z + \frac{2}{3}\Psi^6 \partial^i K. \tag{28}$$

The system we consider is unchanged if it rotates $2\pi/3$ radians around the line $x = y = z$. By virtue of this discrete symmetry, it is enough to solve Eq. (28) for only one component of X^i, since the other two components can be immediately given by this symmetry.

The boundary condition for X^x is given as follows,

$$X^x = 0 \quad \text{on } x = 0 \quad \text{and} \quad x = L, \tag{29}$$

$$\partial_y X^x = 0 \quad \text{on } y = 0 \quad \text{and} \quad y = L, \tag{30}$$

$$\partial_z X^x = 0 \quad \text{on } z = 0 \quad \text{and} \quad z = L. \tag{31}$$

The first condition is the Dirichlet type and the second and third ones are Neumann type boundary conditions. These boundary conditions lead to

$$\int_{\mathcal{D}\text{-}\{O\}} Z \mathrm{d}x^3 = \int_{\mathcal{D}-\{O\}} \partial_i X^i \mathrm{d}x^3 = 0. \tag{32}$$

The above equation is a consistency condition that the solutions should satisfy.

It should be noted that the integrals of the source terms of the Poisson Eqs. (27) and (28) over $\mathcal{D}\text{-}\{O\}$ should vanish by the consistency with the periodic boundary conditions and the boundary condition at the origin O. We can see that these conditions are automatically satisfied. The integral of the source term of Eq. (27) is equivalent to the surface integral over the spatial infinity at O, whereas K vanishes in the neighborhood of O. Hence the integral of the source term of Eq. (27) vanishes. Since $\partial^x Z$ and $\Psi^6 \partial^x K$ are odd functions of x, we have

$$\int_{-L}^{+L} \mathrm{d}x \left(-\frac{4}{3}\partial^x Z + \frac{1}{3}\Psi^6 \partial^x K \right) = 0. \tag{33}$$

Hence, the integral of the x-component of the source term of Eq. (28) vanishes. The same is true for the other components of Eq. (28).

F. Numerical procedure

As shown in the preceding section, we have to solve the following three coupled Poisson equations,

$$\triangle \psi = \triangle\left(\frac{M}{2R}W(R)\right) - \frac{1}{8}(\tilde{L}X)_{ij}(\tilde{L}X)^{ij}\Psi^{-7} + \frac{1}{12}K^2\Psi^5,$$

$$\triangle Z = \frac{1}{2}\partial_i(\Psi^6 \partial^i K), \qquad \triangle X^i = -\frac{1}{3}\partial^i Z + \frac{2}{3}\Psi^6 \partial^i K.$$

In order to get numerical solutions of the above equations, we adopt the method of finite differentiations. By replacing all derivative terms by finite differences, we have a very large simultaneous equation. We solve this simultaneous equation by the Successive Over-Relaxation method. We denote the values of ψ, Z and X^i at each iteration step by $\psi_0, \psi_1, \psi_2 \ldots$, and so on, where the subscript 0 denotes a trial value. At the $(n+1)$-th step of the iteration, the terms corresponding to the source terms of the Poisson equations are estimated by using ψ_n, Z_n and X^i_n.

If we complete the n-th step of the iteration, we obtain Z_n which satisfies the boundary conditions (29)–(31). Here, we should note that this Z_n does not necessarily satisfy the consistency condition (32). In order to obtain Z_n which satisfies Eq. (32), we can use the degree of freedom to add a constant to Z as follows,

$$Z \to Z' := Z - \frac{1}{L^3}\int_{\mathcal{D}\text{-}\{O\}} \mathrm{d}x^3 Z. \tag{34}$$

Z' is also a solution of Eq. (27) and further satisfies Eq. (32), if Z is a solution of Eq. (27). Thus, before evaluating the source term, we reset the value of Z_n as follows:

$$Z_n \to Z'_n = Z_n - \frac{1}{L^3}\int_{\mathcal{D}\text{-}\{O\}} \mathrm{d}x^3 Z_n. \tag{35}$$

It should also be noted that the boundary conditions already given are not enough to close the simultaneous equation, since these boundary conditions do not determine homogeneous solutions of the Poisson equations for ψ and X^i, i.e., their zero modes. (The zero mode of Z is already fixed by Eq. (35).) For this purpose, we need to specify the values of ψ and X^i at one of all numerical grids. We fix the zero modes of ψ and X^i so that $\psi(0) = 1$ and $X^i(0) = 0$, or in other words, before evaluating the source terms, we add constants to ψ_n and X^i_n as

$$\psi_n(\boldsymbol{x}) \to \psi'_n(\boldsymbol{x}) := \psi_n(\boldsymbol{x}) - \psi_n(0) + 1, \tag{36}$$

$$X^i_n(\boldsymbol{x}) \to X'^i_n(\boldsymbol{x}) := X^i_n(\boldsymbol{x}) - X^i_n(0). \tag{37}$$

Note that $\psi(0) = 1$ is equivalent to the choice of $\Psi_c = 1$ in Eq. (15). Eventually, we evaluate the source terms by using ψ'_n, Z'_n and X'^i_n instead of ψ_n, Z_n and X^i_n. The value of H_{eff} is also evaluated through Eq. (23) by using ψ'_n, Z'_n and X'^i_n so that the integrability condition is satisfied.

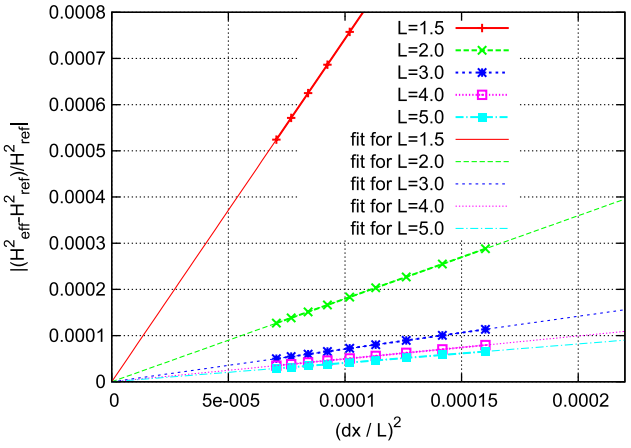

FIG. 3 (color online). Results of convergence test.

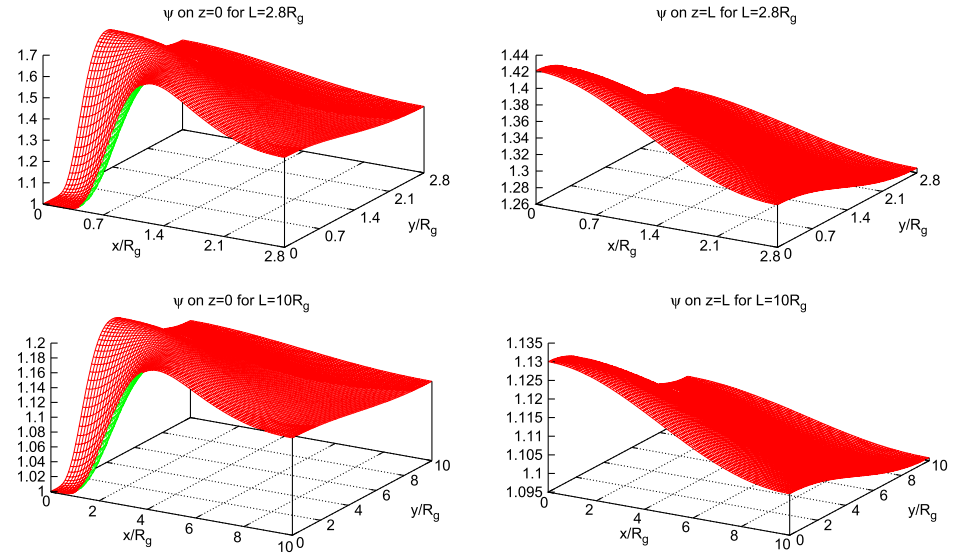

FIG. 4 (color online). ψ on $z = 0$ and $z = L$ planes as functions of x and y for $L = 2.8R_{\rm g}$ and $L = 10R_{\rm g}$.

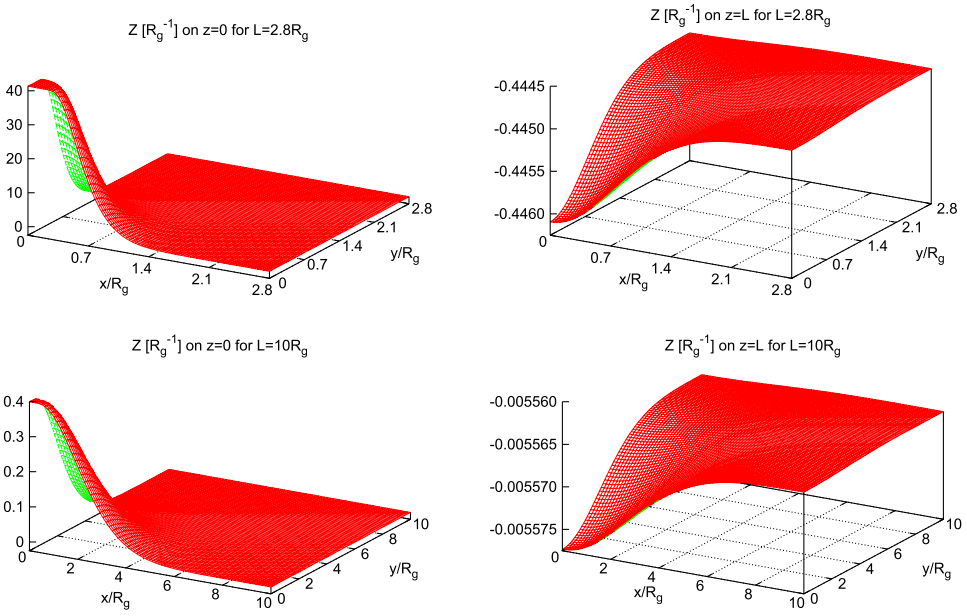

FIG. 5 (color online). Z on $z = 0$ and $z = L$ planes as functions of x and y for $L = 2.8R_{\rm g}$ and $L = 10R_{\rm g}$.

G. Results

We solved the constraint equations in the parameter domain $2.8R_{\rm g} \le L \le 20R_{\rm g}$, where

$$R_{\rm g} := \frac{M}{2}. \tag{38}$$

As will be shown later, the horizons of a black hole are located at $R \simeq R_{\rm g}$. The parameters σ and ℓ which determine K are set to be $\sigma = 0.2R_{\rm g}$ and $\ell = L - 0.4R_{\rm g}$. We could not get convergence for L smaller than $2.8R_{\rm g}$. This result implies that there is no solution for $L < 2.8R_{\rm g}$ on our assumptions: conformally flat metric and no transverse-traceless part of the extrinsic curvature. The results of the convergence test for each value of $L/R_{\rm g}$ are shown in Fig. 3. The second order convergence is confirmed in all cases for the value of $H^2_{\rm eff}$ where the reference value $H^2_{\rm ref}$ is given by the least-square fit. We plot ψ, Z and X^x on $z = 0$ and $z = L$ planes as functions of x and y for $L = 2.8R_{\rm g}$ and $L = 10R_{\rm g}$ in Figs. 4–6.

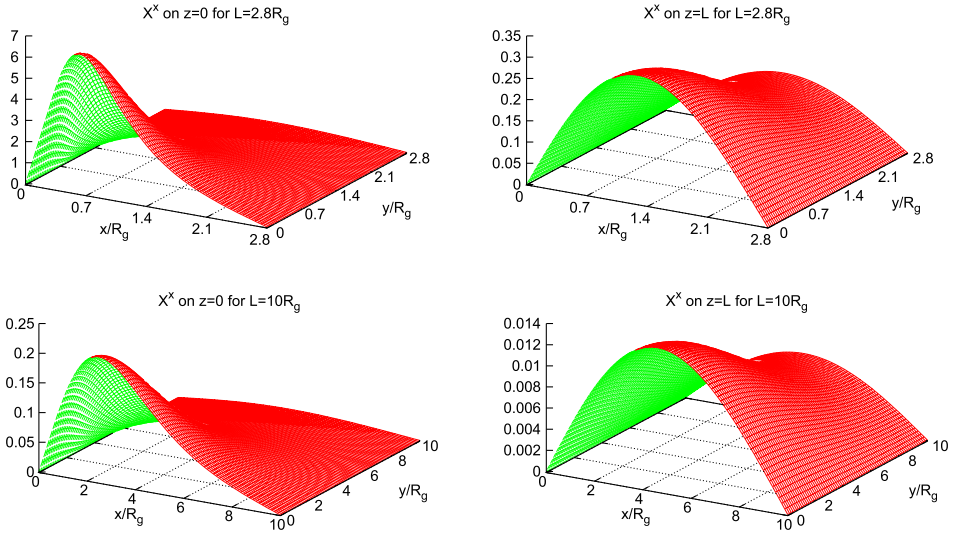

FIG. 6 (color online). X^x on $z = 0$ and $z = L$ planes as functions of x and y for $L = 2.8R_g$ and $L = 10R_g$.

III. ANALYSIS OF THE INITIAL DATA

A. Inhomogeneities

First, we demonstrate the inhomogeneities of our initial data. For this purpose, we investigate the following quantity:

$$\beta := \frac{\gamma^{ac}\gamma^{bd}\mathcal{R}^{\mathrm{T}}_{ab}\mathcal{R}^{\mathrm{T}}_{cd}}{\gamma^{ik}\gamma^{jl}\mathcal{R}_{ij}\mathcal{R}_{kl}}, \tag{39}$$

where $\mathcal{R}_{ij}$ and $\mathcal{R}^{\mathrm{T}}_{ij}$ denote the 3-dimensional Ricci curvature tensor and its traceless part, respectively. We use β as a measure of homogeneity and isotropy, since a region with $\beta = 0$ and $\partial_i\mathcal{R} = 0$ is homogeneous and isotropic. Since we are interested in the inhomogeneities far from black holes, we plot the value of β on $z = L$ plane, which is one of the faces of the domain $\mathcal{D}$, as a function of x and y in Fig. 7. The quantity β almost vanishes in the vicinity of a vertex $x = y = z = L$. Further, the norm of the traceless part of the extrinsic curvature $\Psi^{-12}(\tilde{L}X)_{ij}(\tilde{L}X)^{ij}$ is much less than the square of the trace part of the extrinsic curvature K^2 in the neighborhoods of the vertices. We find from the Hamiltonian constraint together with this fact that $\mathcal{R} \simeq -K^2 = \text{constant}$ and hence $\mathcal{R}_{ij} \simeq -3H^2_{\mathrm{eff}}\gamma_{ij}$, in these regions. Thus, the neighborhoods of the vertices are well approximated by the Milne universe model which is the Minkowski spacetime foliated by the family of homogeneous and isotropic spacelike hypersurfaces with a negative Ricci curvature scalar. Conversely, around the center of a face of $\mathcal{D}$ ($x = y = 0$ and $z = L$), the inhomogeneity remains even if $L \gg R_g$. We may understand this result as follows. If the neighborhoods of all faces of $\mathcal{D}$ were well approximated by the Milne universe model, a 3-hyperboloid would be tiled with the lattice structure shown in Fig. 1. However, this consequence conflicts with a mathematical theorem about "tiling"[4,18].

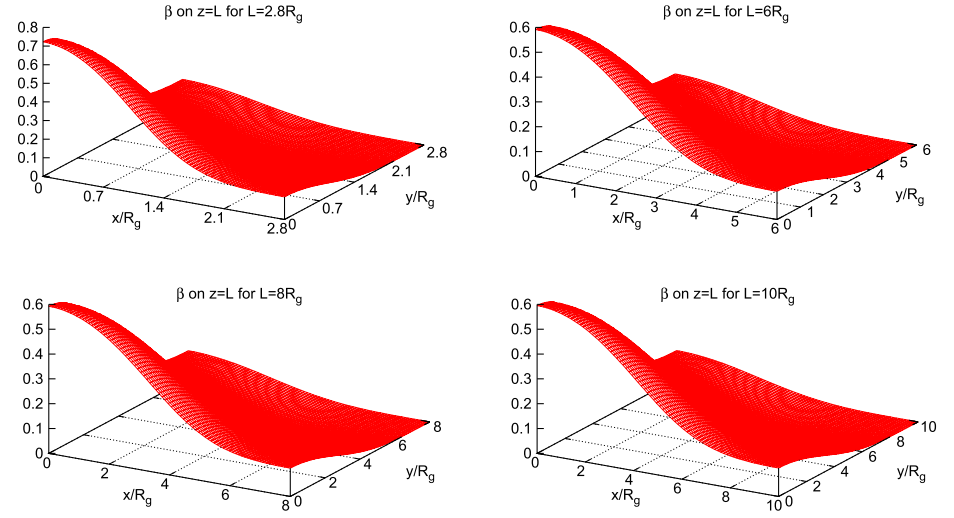

FIG. 7 (color online). β on $z = 0$ and $z = L$ planes as functions of x and y for $L = 2.8R_g$ and $L = 10R_g$.

Therefore, our initial data cannot be homogeneous and isotropic in the neighborhoods of all faces of $\mathcal{D}$ even for $L \gg R_g$ as is explicitly shown in Fig. 7.

B. Horizons

We define a horizon as a spacelike closed 2-surface with vanishing expansion of a null vector field normal to the 2-surface. There are two independent null directions normal to the 2-surface, so there are two kinds of horizons accordingly. Here, we consider these horizons in the domain $\mathcal{D}$-$\{O\}$. A closed 2-surface divides the domain $\mathcal{D}$-$\{O\}$ into two regions. In this paper, since we are interested in the horizons associated with a black hole, we focus on a case in which one of the two regions includes the puncture. We call the domain including the puncture the *inside*, whereas the other domain is called the *outside*. Then, we call the direction from a point on a closed 2-surface to the outside the *outgoing* direction, whereas the opposite direction is called *ingoing* direction. Accordingly, we name a horizon with vanishing expansion of the outgoing null vector field the black hole (BH) horizon, whereas a horizon with vanishing expansion of the ingoing null vector field is named the white hole (WH) horizon.

The expansions of the null vector fields normal to this 2-surface are given by

$$\chi_\pm = (\gamma^{ij} - s^i s^j)(\pm D_i s_j - K_{ij}), \tag{40}$$

where the subscript $+$ means that of the outgoing null, whereas the subscript $-$ represents that of the ingoing null, and s^i is the outgoing unit vector which is normal to this 2-surface and tangent to the initial hypersurface. Defining $\tilde{s}^i$ and $\tilde{s}_i$ as

$$\tilde{s}^i := \psi^2 s^i, \qquad \tilde{s}_i := \delta_{ij}\tilde{s}^j, \tag{41}$$

we rewrite $\chi_\pm$ in the form

$$\chi_\pm = (\tilde{s}_i\tilde{s}_j - \delta_{ij})\left[\Psi^{-6}(\tilde{L}X)^{ij} + \frac{1}{3}\delta^{ij}K\right] \pm \Psi^{-2}\partial_i\tilde{s}^i \pm 4\Psi^{-2}\tilde{s}^i\partial_i \ln\Psi. \tag{42}$$

In this paper, instead of solving the equation $\chi_\pm = 0$, we investigate the expansions of the null vector fields normal to various spheres centered at the origin O. The conformal unit vector $\tilde{s}^i$ normal to the sphere of the radius R is given by

$$\tilde{s}^i = \frac{x^i}{R}. \tag{43}$$

If the initial hypersurface is almost spherically symmetric near the horizon, the horizon is also almost spherically symmetric and $\tilde{s}^i$ is a good approximation of the unit vector field normal to the horizon. In Fig. 8, we plot the expansions $\chi_\pm$ as functions of R on the following three lines:

$$\text{(i)}\ y = 0, z = 0, \qquad \text{(ii)}\ x = y, z = 0, \qquad \text{(iii)}\ x = y = z.$$

From these figures, we see that there are spheres which are very good approximations of horizons; the expansion χ_+ or χ_- at the intersections of these spheres and the lines (i)–(iii) vanishes. The coordinate radius R of the BH horizon is equal to $1.14R_g$ in the case of $L = 2.8R_g$, whereas it is equal to R_g in the case of $L = 10R_g$. The coordinate radius R of the WH horizon is equal to $0.92R_g$ in the case of $L = 2.8R_g$, whereas it is equal to R_g in the case of $L = 10R_g$. In the case of $L = 2.8R_g$, the WH horizon is located inside the BH horizon. Since the domain $R \lesssim R_g$ is well approximated by the Schwarzschild BH, we can say that the initial hypersurface is passing through the future of the bifurcation point of the horizons for $L = 2.8R_g$. On the other hand, in the larger L cases, since the WH and BH horizons coincide with each other, we may say that the initial hypersurface is passing through a domain very close to the bifurcation point.

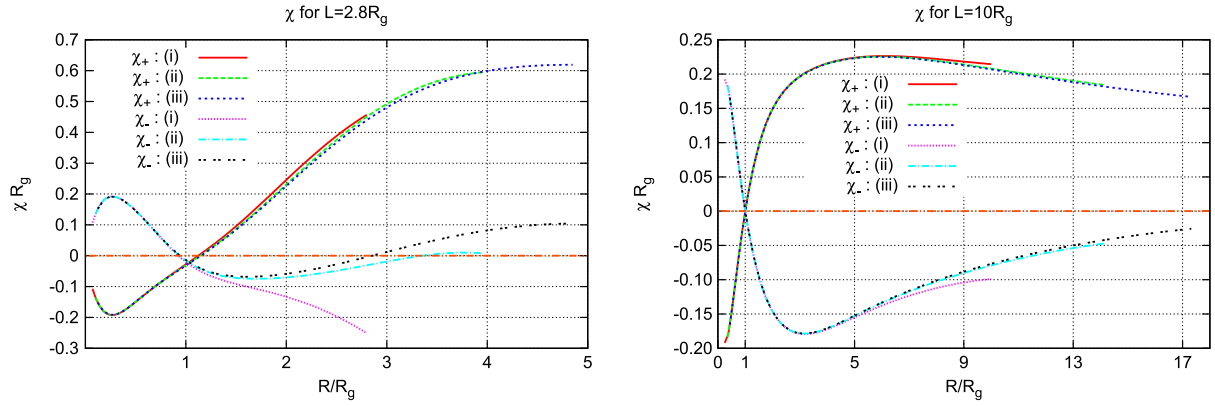

FIG. 8 (color online). $\chi_\pm$ as functions of R for $L = 2.8R_g$ and $L = 10R_g$.

C. Effective Hubble equation

The mass density of black holes $\rho_{\rm H}$ defined by Eq. (24) is roughly estimated at about $M/8L^3$. If the kinetic energy density $\rho_{\rm K}$ defined by (25) is much less than $\rho_{\rm BH}$, the effective Hubble parameter $H_{\rm eff}$ is roughly estimated at about $H_{\rm eff}^2 \sim 8\pi\rho_{\rm BH}/3 \sim \pi M/3L^3$. Then, in the covering space of the domain $\mathcal{D}$-$\{O\}$, the number $N_{\rm BH}$ of black holes within a sphere of the cosmological horizon radius $H_{\rm eff}^{-1}$ is about

$$N_{\rm BH} \sim \frac{1}{M} \times \frac{4\pi}{3} H_{\rm eff}^{-3} \rho_{\rm BH} \sim \frac{1}{4}\left(\frac{3L^3}{2\pi R_{\rm g}^3}\right)^{1/2}. \tag{44}$$

If $L/R_{\rm g}$ is much larger than unity, there are many black holes within a sphere of the cosmological horizon radius, and thus the black hole universe would be very similar to the Einstein-de Sitter (EdS) universe.

From the above consideration, we expect that the effective Hubble parameter and the mass density of black holes asymptotically satisfy the Hubble equation of the EdS universe in the limit of $L/R_{\rm g} \to \infty$. That is, we expect that the effective Hubble parameter behaves asymptotically as

$$H_{\rm eff}^2 \to \frac{8\pi}{3}\rho_{\rm BH}. \tag{45}$$

This means that the contribution of $\rho_{\rm K}$ decreases with larger $L/R_{\rm g}$. We depict $\rho_{\rm K}/\rho_{\rm BH}$ as a function of $L/R_{\rm g}$ in Fig. 9. It is seen from this figure that $\rho_{\rm K}/\rho_{\rm BH}$ asymptotically vanishes for large $L/R_{\rm g}$ and the effective Hubble equation approaches that of the EdS universe.

It is suggestive to regard the one-parameter family of the initial data sets as a fictitious time evolution of the black hole universe. Equation (23) gives the effective Hubble parameter at each time of the fictitious evolution. If we define an effective scale factor by

$$a_V := V^{1/3}, \tag{46}$$

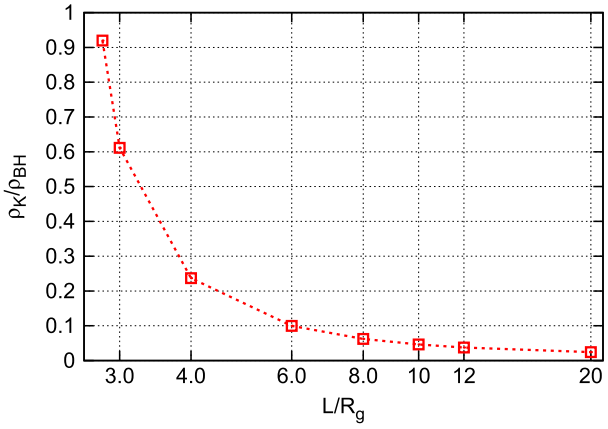

FIG. 9 (color online). $\rho_{\rm K}/\rho_{\rm BH}$ as a function of $L/R_{\rm g}$.

Eq. (45) means that $H_{\rm eff}^2$ asymptotically behaves as $\propto 1/a_V^3$ when the universe expands enough.

Other remarkable ways to define effective scale factors are to use the proper area of the boundary and the proper length of the edge of the cubic domain $\mathcal{D}$. Let a_A and a_L denote the effective scale factors defined by using the proper area and the edge length, respectively. a_L is defined by the proper length of a edge itself and a_A is defined by

$$a_A := \sqrt{\frac{A}{6}}, \tag{47}$$

where A is the proper area of $\partial\mathcal{D}$. In addition, we define the fiducial scale factor $a_{\rm EdS}$ by using the Hubble equation of the EdS universe as follows:

$$a_{\rm EdS}^3 := \frac{8\pi}{3H_{\rm eff}^2}. \tag{48}$$

The relation between effective scale factors and the effective Hubble parameter is shown in Fig. 10. All effective scale factors asymptotically behave as $\propto H_{\rm eff}^{-2/3}$ for larger $L/R_{\rm g}$, that is, the behavior of the effective Hubble parameter as a function of an effective scale factor agrees with that of the EdS universe at late time of the fictitious time evolution. We note that, even though all effective scale factors are asymptotically proportional to $H_{\rm eff}^{-2/3}$, the proportionality coefficients are different from each other. It seems that the proportionality coefficient for a_V asymptotically agrees with that for $a_{\rm EdS}$, but it is not true for a_A and a_L (see the right panel of Fig. 10).

D. Comparison with the Newtonian approximation and backreaction effect

One possible way of approximation which considerably reduces the numerical effort is the cosmological Newtonian approximation. The cosmological N-body simulation based on this approximation scheme is very useful to study the structure formation in the universe indeed. The N-body simulation follows the motion of point particles gravitationally interacting with each other, and these particles are regarded as the dark matter in the cosmological context. The black hole is a candidate for the ingredient of the dark matter in our universe. However, since the black hole is a highly relativistic object, it is nontrivial whether the dark matter composed of black holes is well described by the cosmological N-body simulation based on the Newtonian approximation. Our black hole universe model is a relativistic version of the cosmological N-body system, and thus, by using this model, we can see in what situation the Newtonian N-body simulation correctly describes the motion of the dark matter composed of black holes.

In the cosmological Newtonian approximation scheme, the gravitational force is given by the spatial gradient of the Newtonian potential Φ which is related to the conformal

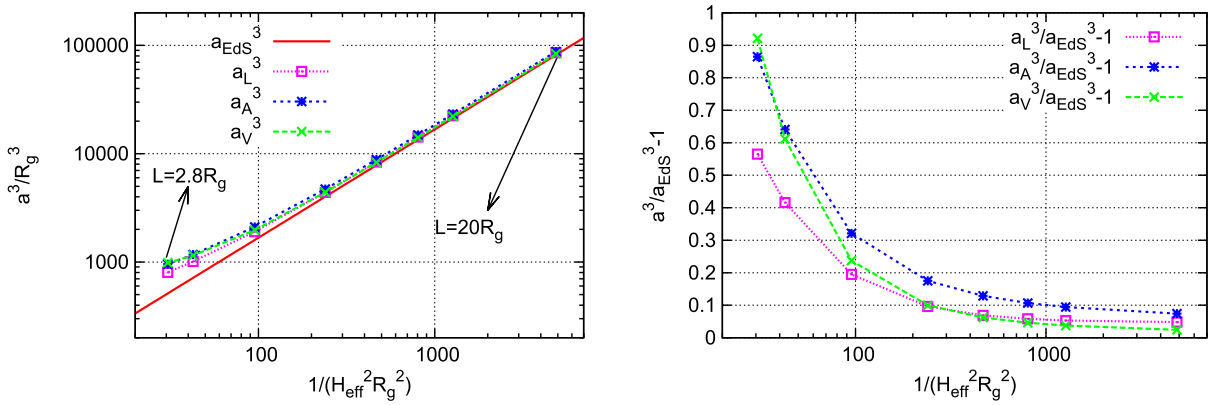

FIG. 10 (color online). Effective scale factors (left panel) and deviations of them from the fiducial scale factor a_{EdS} y (right panel) as functions of the effective Hubble parameter.

factor Ψ by $1-2\Phi=\Psi^4$, and thus the Newtonian potential is obtained by solving the Hamiltonian constraint, which gives the Hubble equation after averaging. Since the metric is assumed to be almost equal to that of the EdS universe model, the term proportional to $(\tilde{L}X)_{ij}(\tilde{L}X)^{ij}$ should be so small that it is a negligible higher order correction in the Hamiltonian constraint. Hence, we do not need to solve the momentum constraint.

Before considering a point particle as the ingredient of the N-body simulation, we assume that the particle is a spherical ball with the finite energy density $\rho(\boldsymbol{x})$. Further, we assume the similar situation to our black hole universe; the particle has the mass M, the center of the particle is located at the origin O in the cubic domain $\mathcal{D}$ whose edge length is $2L$, and the periodic boundary condition is imposed. By definition, we have

$$M=\int_{\mathcal{D}}\rho(\boldsymbol{x})d^3\boldsymbol{x}. \tag{49}$$

The time slicing condition up to the Newtonian order is assumed to be

$$K=-3H_{\mathrm{N}}, \tag{50}$$

where H_{N} is the effective Hubble parameter up to the Newtonian order and is determined by

$$H_{\mathrm{N}}^2=\frac{8\pi}{3}\times\frac{M}{8L^3}. \tag{51}$$

Here note that H_{N} is the same as the Hubble parameter of the background EdS universe model. Then, since nonlinear terms with respect to Ψ in the Hamiltonian constraint are linearized with respect to Φ, the Hamiltonian constraint takes the following form in the cosmological Newtonian scheme [19,20]:

$$\triangle\Phi=4\pi\left[\rho(\boldsymbol{x})-\frac{M}{8L^3}\right]. \tag{52}$$

In the cosmological Newtonian approximation scheme, ρ can be much larger than $M/8L^3$, but ρ should be so small that $|\Phi|$ is much smaller than unity.

Let us consider the case in which the size of the particle is much smaller than L. In this case, since the tidal force can be neglected, it is enough to consider the energy density for a point-particle given by $M\delta(\boldsymbol{x})$ instead of the finite energy density $\rho(\boldsymbol{x})$. Using this approximation, we can accurately estimate the gravitational force produced by a particle at points of other particles. Then the Hamiltonian constraint in the cosmological N-body system is given by

$$\triangle\Phi=4\pi M\delta(\boldsymbol{x})-\frac{\pi M}{2L^3}. \tag{53}$$

Equation (53) is the basic equation for the cosmological N-body simulation based on the Newtonian approximation scheme.

In our case, since the Ψ diverges at O in the black hole universe, it is obvious that the cosmological Newtonian approximation is not applicable in whole region of $\mathcal{D}$-$\{O\}$. When we compare the black hole universe with the cosmological Newtonian system given by Eq. (53), the point-particle approximation, i.e., $\rho(\boldsymbol{x})=M\delta(\boldsymbol{x})$, should be regarded as a technical simplification. Hence, it is a very nontrivial issue whether a point-particle in the cosmological Newtonian N-body system may be identified with a black hole.

In order to numerically obtain solutions of Eq. (53), we decompose Φ as follows:,

$$\Phi=\phi-\frac{M}{R}\Big[1-W(R)\Big]. \tag{54}$$

The equation for ϕ is given by

$$\triangle\phi=-\triangle\left(\frac{M}{R}W(R)\right)-\frac{\pi M}{2L^3}. \tag{55}$$

This can be numerically integrated in $\mathcal{D}$-$\{O\}$ by using the same method as in Sec. II F.

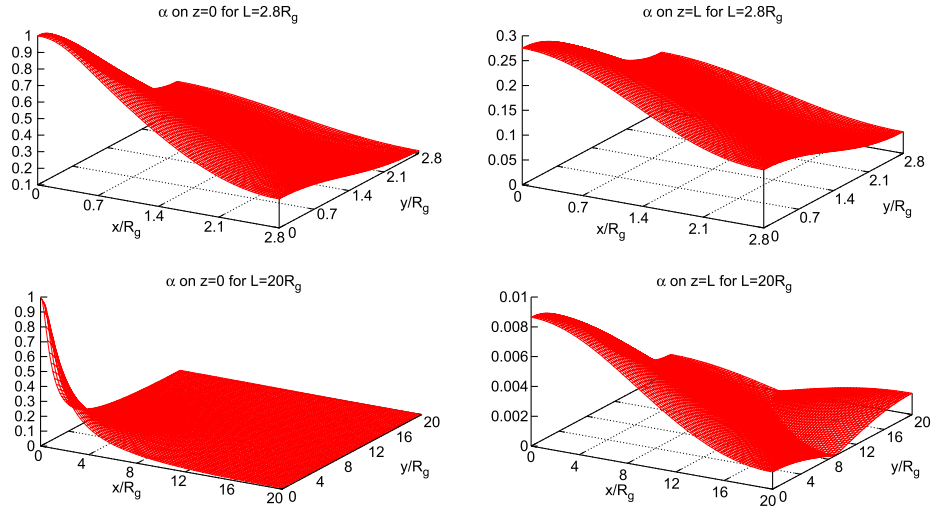

FIG. 11 (color online). α on $z = 0$ and $z = L$ surfaces for $L = 2.8R_g$ and $L = 20R_g$.

To show the deviation of the solution obtained by the cosmological Newtonian approximation from the corresponding relativistic one, we plot the following quantity:

$$\alpha := \left| \frac{\Psi^4 - 1 + 2\Phi}{\Psi^4} \right|. \tag{56}$$

In Fig. 11, α is plotted as a function of the coordinates x and y on $z = 0$ and $z = L$ planes for $L = 2.8R_g$ and $L = 20R_g$, respectively. We can see that while the deviation around the boundary of $\mathcal{D}$ is a few tens of percent for $L = 2.8R_g$, it is less than 1% for $L = 20R_g$. This result implies that the cosmological Newtonian approximation predicts the spatial metric around the boundary of $\mathcal{D}$ very accurately for $L \geq 20R_g$.

As mentioned, the effective Hubble parameter H_N defined by Eq. (51) agrees with that of the background Einstein-de Sitter universe model. The so-called *backreaction* effect is the change of the Hubble parameter from the background value due to the nonlinear effect of the inhomogeneities. Thus, in the present case, we call the effect which causes a difference between the full relativistic Hubble parameter $H_{\rm eff}$ and the background value H_N the backreaction effect.

To see the significance of the backreaction effect, we compare $H^2_{\rm eff}$ to H^2_N with fixed L/R_g. As a result of the numerical investigation, we find that H^2_N has about 20% deviation from $H^2_{\rm eff}$ even for $L = 20R_g$. We plot the value of $1 - H^2_{\rm eff}/H^2_N$ as a function of L/R_g in Fig. 12. It is worthwhile to notice that the Newtonian Hubble parameter is larger than the relativistic one. This means that the backreaction effect acts as the brake in the black hole universe model. Further, our result means that, in the case of $L \leq 20R_g$, the backreaction effect is so large that the cosmological Newtonian approximation cannot predict correctly the global cosmic volume expansion rate. However, Fig. 12 suggests that the deviation of H_N from $H_{\rm eff}$ decreases with larger L/Rg, and hence it seems that the Newtonian N-body simulation becomes correct asymptotically for $L/R_g \to \infty$.

As already shown, in the case of $L = 20R_g$, the relative difference in the spatial metric between the Newtonian scheme and the full relativistic one is a few percents on the boundary of $\mathcal{D}$, and hence the relative differences in the length of an edge and the area of a face are also a few percents. Furthermore, $\rho_{\rm K}$ defined by Eq. (25) is about 2% of $\rho_{\rm BH}$ (see Fig. 9). Thus, the difference between $H^2_{\rm eff}$ and H^2_N comes from the difference between the volume V defined by Eq. (22) and $8L^3$; V is about 1.3 times larger than $8L^3$.

Here, we should note that the backreaction effect is large even in the case of $L = 20R_g$, but, as shown in the preceding section, the expansion law of the black hole universe model might be almost the same as that of the EdS universe. These results would imply that the backreaction

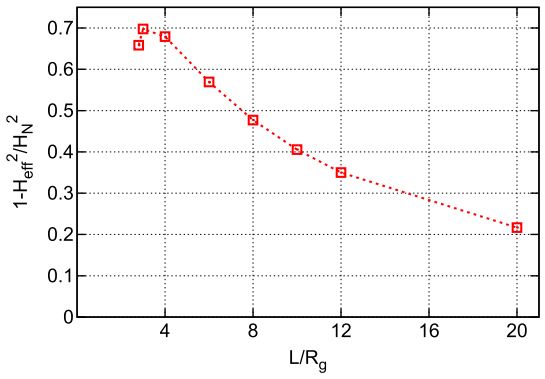

FIG. 12 (color online). $1 - H^2_{\rm eff}/H^2_N$ as a function of L/R_g.

effect in the black hole universe model would not change the expansion law from the EdS universe model but apparently shifts the time to the future. However, in order to get a definite conclusion, the investigation of the time evolution is necessary.

IV. SUMMARY AND CONCLUSION

In this paper, we have constructed numerically the initial data of an expanding universe model which is composed of regularly aligned black holes. This system is equivalent to a black hole located at the center O of a cubic domain $\mathcal{D}$ with periodic boundary conditions. The black hole is represented by a structure like the Einstein-Rosen bridge, and thus O corresponds to the asymptotically flat spatial infinity. Since the physical domain does not include infinity, the physical domain is $\mathcal{D}$ with O removed, i.e., $\mathcal{D}$-$\{O\}$ whose topology is $\mathbf{T}^3$ with one point removed. The functional form of the trace of the extrinsic curvature $K(\boldsymbol{x})$ has been chosen so that K is a negative constant denoted by $-3H_{\rm eff}$ in the neighborhoods of the faces of $\mathcal{D}$ and vanishes in the neighborhood of O, where $H_{\rm eff}$ corresponds to the effective Hubble parameter. These requirements are compatible with a finite expansion rate of the universe and the puncture method to numerically treat a black hole, respectively. Then, we can solve constraint equations by giving the parameter $L/R_{\rm g}$, where L is the coordinate length of an edge of the cubic domain $\mathcal{D}$, and $R_{\rm g}$ gives a coordinate value which is almost equal to the coordinate radius of the black hole horizon. The value of $H_{\rm eff}$ is determined so that the integral of the Hamiltonian constraint over $\mathcal{D}$-$\{O\}$ is compatible with the periodic boundary conditions; this integral leads to the effective Hubble equation. We find from numerically obtained solutions that the neighborhoods of vertices of $\mathcal{D}$ are well approximated by the Milne universe, whereas the other region remains inhomogeneous even in the case of $L \gg R_{\rm g}$. This result implies that the initial data of the black-hole universe model is inhomogeneous even near the faces of $\mathcal{D}$ irrespective of the value of $L/R_{\rm g}$.

We could find one white hole and one black hole horizon in the present initial hypersurface of $\mathcal{D}$-$\{O\}$, and both are almost spherically symmetric. This result implies that the region $R \lesssim R_{\rm g}$ is well approximated by the Schwarzschild black hole, and the initial hypersurfaces considered here are passing through the future of the bifurcation point of the horizons or a very close point to it.

In order to compare our initial data with the Einstein-de Sitter (EdS) universe, we studied the relation between the effective mass density $\rho_{\rm BH}$ of black holes and the effective Hubble parameter $H_{\rm eff}$, which are defined in a simple and natural way. Then, our numerical solutions imply that $\rho_{\rm BH}$ and $H_{\rm eff}$ asymptotically satisfy the Hubble equation of the EdS universe for $L \gg R_{\rm g}$. Once we regard our one-parameter family of initial data sets as a fictitious time evolution of the black hole universe, our result would imply that the Hubble equation of the EdS universe would be realized when the universe expands enough.

The validity of the Newtonian approximation in the system has also been discussed. We numerically solved the Hamiltonian constraint equation simplified by the cosmological Newtonian approximation and compared it with the full solution with fixed $L/R_{\rm g}$. We found that the deviation of the spatial metric obtained by the cosmological Newtonian approximation from that of the full calculation is less than 1% for $L/R_{\rm g} = 20$ around the boundary of $\mathcal{D}$ and better for larger values of $L/R_{\rm g}$. However, the deviation of the Hubble parameter defined in the cosmological Newtonian approximation scheme and full relativistic one is 20% even for $L/R_{\rm g} = 20$. Thus, we may say that, as expected, the backreaction effects of the inhomogeneities on the cosmic volume expansion are very large in the case of $L \leq 20R_{\rm g}$. However, we may also say that, for the larger $L/R_{\rm g}$, the backreaction effects become smaller. It is worthwhile to notice that the backreaction effect acts as the brake for the cosmic volume expansion.

Here we note that all our results might depend on the assumptions which have been made in Secs. II A and II B. Since we have not solved the evolution equation, we cannot address the real time evolution of the black hole universe at all. Therefore, it is not clear if the dynamics of the black hole universe can be described by the EdS universe on average or not. One should keep in mind that the black hole universe cannot be exactly the EdS universe and the effect of inhomogeneities definitely exists. The effect of the inhomogeneities might give a qualitative difference of the global expansion history of the universe [8,9,21,22]. By contrast, the present results would imply that the backreaction effect would not change the expansion law of the black hole universe from that of the EdS universe model; the backreaction effects might merely shift the time to the future. To attack this issue we need further numerical efforts, and we leave it as a future work.

ACKNOWLEDGMENTS

We thank H. Okawa, T. Shibata, T. Tanaka, M. Sasaki and N. Yoshida for helpful discussions and comments. The numerical calculations were carried out on SR16000 at YITP in Kyoto University. C. Y. is supported by a Grant-in-Aid through the Japan Society for the Promotion of Science (JSPS). The authors thank the Yukawa Institute for Theoretical Physics at Kyoto University. Discussions during the YITP workshop YITP-T-11-08 on ''Recent advances in numerical and analytical methods for black hole dynamics '' were useful to complete this work. This work was supported in part by JSPS Grant-in-Aid for Scientific Research (C) (No. 21540276).

APPENDIX A: CONSTANT MEAN CURVATURE SLICES IN SCHWARZSCHILD SPACETIME

Let us consider the Schwarzschild spacetime, whose metric is given by

$$\mathrm{d}s^2 = -f(r)\mathrm{d}t^2 + \frac{1}{f(r)}\,\mathrm{d}r^2 + r^2\mathrm{d}\Omega^2, \tag{A1}$$

where

$$f(r) = 1 - \frac{r_{\mathrm{g}}}{r}. \tag{A2}$$

We consider a constant mean curvature (CMC) slice given by the form of

$$t = h(r). \tag{A3}$$

The unit normal vector is given by

$$n^\mu = \frac{1}{\sqrt{f^{-1} - fh'^2}}(f^{-1}, fh', 0,). \tag{A4}$$

The CMC slice condition is given by

$$\begin{aligned}\nabla_\mu n^\mu = -K &\Leftrightarrow \frac{1}{r^2}\partial_r(r^2 n^r) = -K \Leftrightarrow n^r = -\frac{1}{3}Kr + \frac{C}{r^2} \\ &\Leftrightarrow f^{-1}(1 - f^2h'^2) = F(r; r_{\mathrm{g}}, K, C) \\ &:= \frac{1}{1 - \frac{r_{\mathrm{g}}}{r} + (-\frac{1}{3}Kr + \frac{C}{r^2})^2},\end{aligned} \tag{A5}$$

where C is the integration constant. Then, line elements on the CMC slice are given by

$$\mathrm{d}\ell^2 = F(r; r_{\mathrm{g}}, K, C)\mathrm{d}r^2 + r^2\mathrm{d}\Omega^2. \tag{A6}$$

The transformation to the isotropic coordinate can be done as follows:

$$\mathrm{d}\ell^2 = \Psi^4(\mathrm{d}R^2 + R^2\mathrm{d}\Omega^2), \tag{A7}$$

$$R = C\exp\left[\pm\int_{r_{\min}}^{r}\mathrm{d}r\sqrt{F(r; r_{\mathrm{g}}, K, C)}/r\right], \tag{A8}$$

$$\Psi = \sqrt{r/R}, \tag{A9}$$

where $r_{\min}$ is the largest root of $F(r; r_{\mathrm{g}}, K, C) = 0$ and $r = r_{\min}$ corresponds to the throat. The minus sign is used in the region beyond the throat. We can easily check that, in the limit of $r \to \infty$, the isotropic coordinate R has finite value if $K \neq 0$. While $R = 0$ for $r \to \infty$ if $K = 0$. Hence, the coordinate region with R has an inside spherical boundary with $K \neq 0$. This property is not compatible with the puncture method.

[1] A. Einstein and E. G. Straus, Rev. Mod. Phys. **17**, 120 (1945).
[2] A. Einstein and E. Straus, Rev. Mod. Phys. **18**, 148 (1946).
[3] R. W. Lindquist and J. A. Wheeler, Rev. Mod. Phys. **29**, 432 (1957).
[4] T. Clifton and P. G. Ferreira, Phys. Rev. D **80**, 103503 (2009).
[5] J.-P. Uzan, G. F. Ellis, and J. Larena, Gen. Relativ. Gravit. **43**, 191 (2010).
[6] G. F. R. Ellis and W. Stoeger, Classical Quantum Gravity **4**, 1697 (1987).
[7] T. Futamase, Phys. Rev. Lett. **61**, 2175 (1988).
[8] H. Russ, M. H. Soffel, M. Kasai, and G. Borner, Phys. Rev. D **56**, 2044 (1997).
[9] T. Buchert, Gen. Relativ. Gravit. **32**, 105 (2000).
[10] G. F. Ellis and T. Buchert, Phys. Lett. A **347**, 38 (2005).
[11] T. Buchert, Gen. Relativ. Gravit. **40**, 467 (2007).
[12] S. Rasanen, Classical Quantum Gravity **28**, 164008 (2011).
[13] T. Kai, H. Kozaki, K.-i. Nakao, Y. Nambu, and C.-M. Yoo, Prog. Theor. Phys. **117**, 229 (2007).
[14] T. Clifton, K. Rosquist, and R. Tavakol, arXiv:1203.6478.
[15] E. Gourgoulhon, arXiv:gr-qc/0703035, Lecture notes.
[16] C. Hellaby, Classical Quantum Gravity **4**, 635 (1987).
[17] J. Plebanski and A. Krasinski, *An Introduction to General Relativity and Cosmology* (Cambridge University Press, Cambridge, United Kingdom, 2006).
[18] H. M. S. Coxeter, *Regular Polytopes, Book* (Methuen and Company Ltd., London, (1948).
[19] P. J. E. Peebles, *The Large-Scale Structure of the Universe* (Princeton University Press, Princeton, NJ, 1980).
[20] M. Shibata and H. Asada, Prog. Theor. Phys. **94**, 11 (1995).
[21] Y. Nambu, Phys. Rev. D **65**, 104013 (2002).
[22] M. Kasai, H. Asada, and T. Futamase, Prog. Theor. Phys. **115**, 827 (2006).